# BP neural network model for material distribution prediction based on variable amplitude anti-blocking screening DEM simulations

Zheng Ma[1,2,3*], Yongle Zhu[1,2,3], Zhiping Wu[1,2,3], Souleymane Nfamoussa Traore[1,2,3], Du Chen[4], Licheng Xing[5]

(1. *School of Agricultural Engineering, Jiangsu University, Zhenjiang 212013, Jiangsu, China*;
2. *Key Laboratory of Modern Agricultural Equipment and Technology, Ministry of Education & Jiangsu Province, Jiangsu University, Zhenjiang 212013, Jiangsu, China*;
3. *Key Laboratory for Theory and Technology of Intelligent Agricultural Machinery and Equipment, Jiangsu University, Zhenjiang 212013, Jiangsu, China*;
4. *College of Engineering, China Agricultural University, Beijing 100083, China*;
5. *Jiangsu World Agricultural Machinery Co., Ltd., Picheng Industrial Park, Danyang 212311, Jiangsu, China*)

**Abstract:** The material feeding changing of combine harvester is easy to cause accumulation and blockage of the vibrating screen, which seriously affects the harvest operation. In order to alleviate such accumulation and blockages on the vibrating screen surface, the guide chute rotation angle of the improved variable amplitude screening mechanism was selected as the target variable, and EDEM-RecurDyn was employed to simulate the anti-blocking process of the variable amplitude under a changing feeding quantity (0.5 kg/s abnormal, 0.2 kg/s normal) of materials (rice grain and stem mixture). A BP (an error back propagation algorithm) neural network was designed and the prediction model of the material distribution was subsequently constructed on the variable screening surface under different chute angles during abnormal feeding. The results revealed a continuous decrease in the quality and time of the material blockage at the front end of the screen surface with the increasing guide chute angle. At the guide chute angle of 20°-45° and adjustment time of 3-6 s, the blocked and accumulated materials at the front-end screen surface was be moved back to Grid 6 for screening. However, overtime, the screen surface materials continued to move back under the chute angle of 40°-45°, which had a great impact on the screening performance. At the guide chute angle of 30°-35° and adjustment time of 4 s, the materials on the screen surface were evenly distributed in Grid 1-6. This was able to alleviate the accumulation and blockage of the screen surface materials. The $R$ of the material distribution prediction model (BP neural network) on the screen surface was determined as 0.97, indicating the high reliability and accuracy of the material distribution model on the screen surface based on the BP neural network. This work provides an important reference for the variable amplitude intelligent control of screen surface material anti-blocking.

**Keywords:** variable amplitude, material distribution, EDEM-RecurDyn, BP neural network
**DOI:** 10.25165/j.ijabe.20231604.7178

**Citation:** Ma Z, Zhu Y L, Wu Z P, Traore S N, Chen D, Xing L C. BP neural network model for material distribution prediction based on variable amplitude anti-blocking screening DEM simulations. Int J Agric & Biol Eng, 2023; 16(4): 190–199.

## 1 Introduction

The cleaning process is an integral component of crop harvesting. The vibrating screen is an important part of the cleaning link, which uses the principle of vibration to screen materials[1]. Variations in the crop density and operating parameters of the combine may alter the material feeding quantity during the combine harvesting operation. Furthermore, all working links of the combine are closely related, and the vibrating screen in the cleaning link may exhibit low load limit and poor adaptability to other links. This can result in the material accumulation and blockage on the screen surface due to changes in the material feeding quantity, seriously affecting the harvest operation. Thus, improvements must be made to the vibrating screen in order to reduce the risk of material accumulation and blockage on the screen surface.

Numerous studies have investigated the anti-blocking screening of the vibrating screen, including the development of screens with multi degrees of freedom, the optimization of operating parameters, the application of variable amplitude principles etc. The multi-degree-of-freedom screening mechanism is huge, complex, and expensive, and thus it is not suitable for the limited cleaning space of combine harvesters[2-4]. Previous research has demonstrated amplitude and vibration frequency as key factors affecting vibration screening[5,6], yet the adjustment of the latter is not suitable for the fixed and related transmission ratios of the working parts included in the majority of combine harvesters in China. The principle of variable amplitude is based on the boom reciprocating vibrating screen in the combine to dynamic change the length of the front boom and the position of the suspension point. It changes the original parallelogram structure and motion trajectory, resulting in an inconsistent amplitude between the front and rear ends of the

**Received date:** 2021-11-07 **Accepted date:** 2023-03-12
**Biographies: Yongle Zhu**, PhD, research interest: design and theory of modern agricultural machinery, Email: 2017429651@qq.com; **Zhiping Wu**, PhD, research interest: design and theory of modern agricultural machinery, Email: 1524809351@qq.com; **Souleymane Nfamoussa Traore**, MS candidate, research interest: design and theory of modern agricultural machinery, Email: traoresoul53@gmail.com; **Du Chen**, PhD, research interest: Email: tchendu@cau.edu.cn; **Licheng Xing**, Email: xlc15789@163.com.
***Corresponding author: Zheng Ma**, PhD, PhD Supervisor, Associate Research Fellow, research interest: design and theory of modern agricultural machinery. College of Agricultural Engineering, Jiangsu University, Zhenjiang 212013, China. Tel: +86-18796087291, Email: mazheng123@ujs.edu.cn.

screen surface. Under a variable amplitude, the amplitude of the screen surface front end of increases, while that of the rear end decreases. This is able to enhance the throwing strength for the front end of the screen surface due to the accumulation and blockage of materials caused by the increased material feeding quantity[7]. The function of variable amplitude screening is relatively single, namely the materials at the front end of the screen surface disperse and move back quickly. The variable amplitude adjustment is also convenient and is able to effectively alleviate the accumulation and blockage of materials on the screen surface (particularly at the screen surface front end), improving the adaptation ability to other links. In addition, the variable amplitude screening structure is compact and easy to arrange in the limited cleaning space of the combine harvester and is thus worthy of further study.

The discrete element method (DEM) is a simulation approach for particle motion that can generate multiple particles to simulate the vibration screening process under variations in material feeding. DEM has been widely employed in recent years in the field of agricultural material screening, reducing test costs and improving the efficiency[8]. The applications of DEM include the simulation and analysis of the vibrating screening process, the investigation of motion law, the screening and screening mechanism of single and group particles on the vibrating screen[9-12], analyzing the influence of the vibrating screen working parameters on the particle motion and screening performance, and optimizing the vibrating screen working parameters[13-16]. However, DEM is only able to simulate simple motion forms, while complex and adjustable motion forms prove to be too difficult for this approach. In order to overcome this, RecurDyn (multi-body dynamics software) and EDEM (discrete element software) are combined to jointly simulate the vibration screening process of materials[5,17], thus facilitating the regulation of variable amplitude motion. In addition, several scholars have investigated the material distribution of the screen surface for the screening and blocking prevention of vibrating screens[18,19]. However, the accumulation and blockage of materials are typically focus on vibrating screen surface. Thus, there is an urgent demand for an accurate and reliable material distribution model of the screen surface to further optimize its structure and operating parameters and minimize, accumulation and blockages.

Machine learning is a computer technology branch that employs existing data to determine a model and uses this model to predict the future. The integration of neural networks with deep learning is widely used in machine learning due to its capabilities deep self-learning, self-organization, and self-adaptation[20,21]. The BP neural network is a multilayer feedforward neural network trained according to the error back propagation algorithm. The popular BP neural network possesses numerous favorable properties, including a strong nonlinear mapping between input and output, high self-adaptation and self-learning, good fault tolerance, etc. It is also able to establish an accurate and reliable prediction model based on the existing data via self-adaptation and deep self-learning. The BP neural network is widely used in agricultural fields such as automatic control, agricultural machinery power prediction, information decision-making, variable rate fertilization and crop planting, and thus plays an important supporting role in agricultural intelligence[22,23]. Specific applications include the identification of crop varieties and growth status predictions[24-26], optimizing the threshing and screening parameters of materials, and screening performance predictions[27-30]. However, limited studies have employed neural networks to investigate the problem of material accumulation and blockage on the vibrating screen surface under a changing material distribution. Previous work has proposed a vibrating screen particle distribution model based on a biological neural network (BNN)[31], yet this lacks the advantages of self-learning and self-adaptive of the BP neural network. Moreover, the particle through--screen and vibration transportation in the distribution model cannot by efficiently applied to the variable amplitude screen material distribution model.

Although the vibrating screen with variable amplitude principle can effectively alleviate the accumulation and blockage of screen surface materials, there is still a lack of accurate and reliable screen surface material distribution models to further optimize and adjust the variable amplitude. Theoretical analysis (i.e., screening probability and dynamic models) is complex and is not able to fully establish a material distribution model for variable amplitude screen surfaces, and the accuracy of the model is difficult to ensure. In particular, for variable amplitude screen surfaces, the amplitude and vibration direction angle at different positions of the variable amplitude screen surface are different, which results in the inconsistency of the screening probability, moving speed and acceleration of particles at different positions of the screen surface. The BP neural network can establish a relatively accurate and reliable material distribution model based on the existing data via deep self-learning, which is difficult to achieve through theoretical analysis and modeling. More specifically, the EDEM can simulate the variable amplitude screening and blocking prevention process under changing material feeding quantities in order to collect enough distribution data of particle groups on the screen surface. In order to judge the anti-blocking screening effect of variable amplitude adjustment on vibrating screen under abnormal feeding conditions, optimize variable amplitude adjustment and establish variable amplitude adjustment strategy, material distribution model on screen surface is established through RecurDyn-EDEM simulation data and BP neural network. This overcomes the limitations of EDEM simulation and the difficulty of traditional theoretical modeling, and provide an important reference for the future regulation of variable amplitudes to alleviate the accumulation and blockage of screen materials.

## 2 Materials and methods

### 2.1 Variable amplitude principle and screening mechanism

Figure 1 presents the principle of variable amplitude, where AC and BD represent the front boom and rear boom respectively, CD is the vibrating screen, HF is the connecting rod, G is the center of the eccentric wheel, and $\alpha$ is the initial inclination of the vibrating screen. ACDB to AC'D'B in Figure 1 demonstrates the movement process of the reciprocating vibrating screen, whereby the screen surface moved backward, and the amplitude and vibration direction angle of each position of the screen surface did not change. Front boom AC was rotated by a certain angle (maximum 45°) from the vertical state and fixed to the position of A', and thus A'CDB formed a variable amplitude screening mechanism. A'CDB to A'C"D'B reveals a change in the motion state of the vibrating screen at this time. Comparing CD to C'D' and CD to C"D' demonstrates that the initial attitude inclination angle of vibrating screen CD did not change. However, parameters such as the amplitude and vibration direction angle at different positions of screen surface changed, and the amplitude at the screen surface front end was significantly greater than that at the rear end. The principle of variable amplitude is based on changing the length of the front boom and the position of the suspension point via the boom reciprocating vibrating screen to change the original parallelogram

structure and motion trajectory, and to achieve distinct amplitudes at the front and rear ends of the screen surface. More specifically, the amplitude of the front end is enhanced, while the rear end amplitude is reduced. This can alleviate the accumulation and blockage of the materials on the screen surface, which typically occurs at the front end[7].

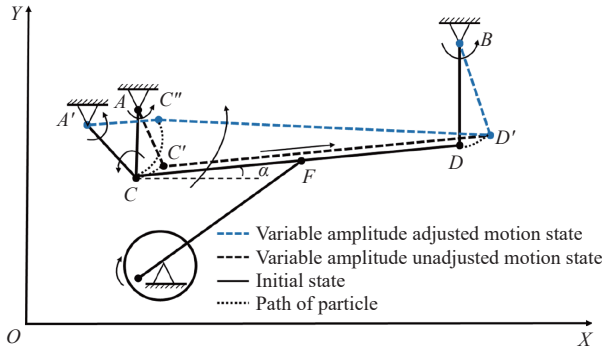


Figure 1 The adjusting screen surface amplitude principle by the variable amplitude screening mechanism.

Figure 2 depicts the improved variable amplitude screening mechanism, which is composed of a hopper, baffle, vibrating screen, guide chute, boom, receiving box, connecting rod, eccentric wheel, and rotating shaft. The length, width and height of the hopper were 200 mm, 100 mm, and 1000 mm respectively, the length, width and height of the vibrating screen were 1000 mm, 200 mm, and 200 mm respectively, and the initial attitude inclination was 4°. Material feeding was realized through the hopper, and the material feeding rate was controlled by the moving speed and moving time of the baffle, allowing for changes in the material feeding quantity. The variable amplitude adjustment was performed by rotating the guide chute at different angles. An increase in the guide chute rotation angle enhanced the initial attitude inclination of the vibrating screen and the amplitude of the screen surface front end, while the amplitude of the rear end decreased. This accelerated the backward movement and dispersion of the materials, making full use of the screen surface, and alleviating the accumulation and blockage of materials at the screen surface front end.

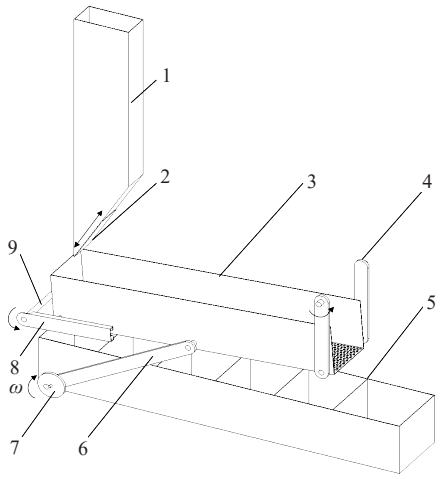


1. Hopper 2. Baffle 3. Vibration sieve 4. Boom 5. Receiving box 6. Connecting rod 7. Eccentric wheel 8. Guide chute 9. Rotating shaft

Figure 2 Three dimensional model of the improved variable amplitude screening mechanism

### 2.2 EDEM-RecurDyn simulation model

Three-dimensional models of rice and stem grains were established through the particle function of EDEM. Some scholars studied the influence of the ratio of ball to powder diameter (BPDR) and the shape of powder particles on the EDEM simulation results and time. The results showed that the size and shape of powder particles would not significantly change the motion mode and simulation results of the ball, and the simulation time and data size increased exponentially with the increase of BPDR[32]. Therefore, a cylindrical rice stem model (Figure 3a) and elliptical rice grain model (Figure 3b) were employed to instead of various sizes particles for simulation according to previous research[9]. SoildWorks was used as the three-dimensional solid model of the variable amplitude screening mechanism. This model was imported into RecurDyn to set the relevant kinematic pairs and driving

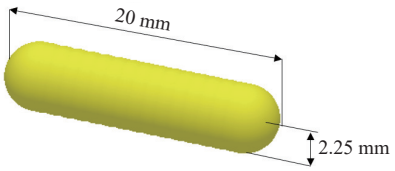


a. Model of rice stem

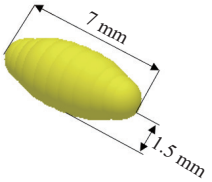


b. Model of rice grain

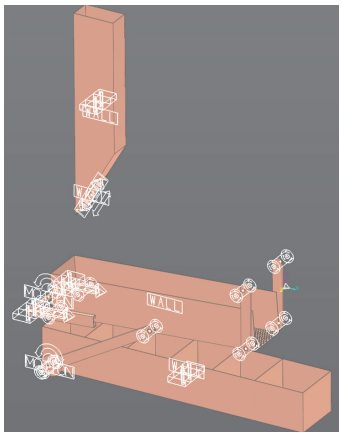

c. Set kinematic model in RecurDyn

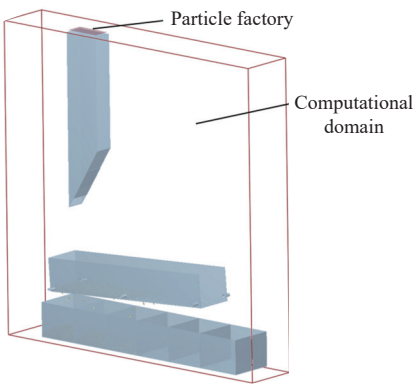


d. Set simulation model in EDEM

Figure 3 Model settings in the variable amplitude screening process

functions. Figure 3c presents the kinematic model of the variable amplitude screening mechanism and the relevant constraints and function settings. The key components (contact with the rice grain and stem particles in EDEM) were set as the WALL format in RecurDyn, and the WALL files were imported into EDEM to set the particle factory, contact model, calculation domain, etc. Figure 3d presents the WALL models and several EDEM settings.

### 2.3 Simulation parameters setting

RecurDyn is a multi-body system dynamics simulation software that can simulate the statics, kinematics, and dynamics of a model. RecurDyn was employed to add the corresponding kinematic pairs and constraints to each three-dimensional model component of the variable amplitude screening mechanism for the subsequent kinematic simulation. Table 1 reports the kinematic pairs and constraint settings of the components for the RecurDyn variable amplitude screening mechanism.

**Table 1 Motion pairs and the constraints of the variable amplitude screening mechanism in RecurDyn.**

| Number | Motion pair | Connector |
|---|---|---|
| 1 | Fixed hinge | Hopper and Ground |
| 2 | Slip hinge | Hopper and Baffle |
| 3 | Rotating hinge | Boom and Ground |
| 4 | Rotating hinge | Boom and Vibrating screen |
| 5 | Rotating hinge | Connecting rod and Vibrating screen |
| 6 | Rotating hinge | Connecting rod and Eccentric wheel |
| 7 | Rotating hinge | Eccentric wheel and Ground |
| 8 | Rotating hinge | Pulley and Vibrating screen |
| 9 | Slip hinge | Pulley and Guide chute |
| 10 | Fixed hinge | Guide chute and Rotating shaft |
| 11 | Rotating hinge | Rotating shaft and Ground |
| 12 | Fixed hinge | Receiving box and Ground |

The driving functions of the variable amplitude screening mechanism were set via RecurDyn (Table 2). STEP (unit step response function) was created, amongst other functions to control the baffle displacement (for material feeding rate changes), the guide chute rotation angle (variable amplitude adjustments), and the eccentric rotational speed (for the vibration frequency control and to drive the variable amplitude screening mechanism). Based on previous work on the optimization of the vibrating screen operating parameters (i.e., the vibration frequency)[33], the vibration frequency of the vibrating screen was set to 5 Hz. For the RecurDyn-EDEM simulations, the variable amplitude screening process under abnormal feeding needs to set the same simulation time and time steps, respectively. The final simulation time was set to 12.6 s: i) the guide chute rotation angle for the variable amplitude screening mechanism was adjusted within 0-2.5 s; ii)the dynamic generation of particles in the EDEM particle factory to fill the hopper with materials was performed within 0-2.5 s; iii) and the opening the hopper outlet baffle to feed materials occurred between 2.5-2.6 s; and iv) the material feeding and variable amplitude screening processes were performed within 2.6-12.6 s.

The rice and stem particle factories were set at 400 mm above the hopper, respectively, for the importation of the WALL model into EDEM. Both particle factories were rectangular, with a length and width of 190 mm and 90 mm, respectively. Following the calculations, the generation rate of the rice and stem was set to 0.475 kg/s and 0.025 kg/s, the total mass to 2.375 kg and 0.125 kg, and the total number of particles to 53 096 and 3499, respectively. This ensured that the rice grain and stem particles could complete the material filling of the hopper within 2.5 s. The relationship between the vertical cross-sectional area of the hopper outlet and the material feeding rate was obtained by fitting the preliminary simulation test data. The STEP function was set in RecurDyn to control the upward moving distance of the baffle, to change the cross-sectional area of the outlet, and to control the change of the feeding rate (e.g., 0.5 kg/s). The no-slip Hertz-Mindlin model was adopted for the contact model between particles, and between particles and numerous components. The predecessors have conducted experimental measurement of relevant parameters [34]. No relevant parameters of rice grains and stems have been measured to reduce the duplication of research work, and only some parameters have been slightly adjusted to improve the calculation efficiency and save simulation time. Table 3 lists the material properties and contact parameters of the rice grain and stem in EDEM.

**Table 2 Set the driving functions of variable amplitude screening mechanism in RecurDyn.**

| Name | Function expression |
|---|---|
| Hopper and baffle | STEP (time,0,0,2.5,0) + STEP (time,2.5,0,2.6, -0.06) + STEP (time,7.6,0,12.6,0) |
| Guide chute | STEP (time,0,0d,2.5, -5d) + STEP (time,2.5,0d,12.6,0d) |
| Eccentric wheel | 10PI |

**Table 3 Material properties and contact parameters of particles in EDEM.**

| Item | Attribute | Numerical value |
|---|---|---|
| Rice grain | Poisson's ratio | 0.3 |
| | Shear modulus/Pa | $2.6\times10^{6}$ |
| | Density/kg·m$^{-3}$ | 1350 |
| Rice stem | Poisson's ratio | 0.4 |
| | Shear modulus/Pa | $1\times10^{6}$ |
| | Density/kg·m$^{-3}$ | 100 |
| Variable amplitude screening mechanism | Poisson's ratio | 0.3 |
| | Shear modulus /Pa | $7\times10^{8}$ |
| | Density /(kg·m$^{-3}$) | 7850 |
| Rice grain-Rice grain | Restitution coefficient | 0.2 |
| | Static friction coefficient | 1.0 |
| | Dynamic friction coefficient | 0.01 |
| Rice grain-Rice stem | Restitution coefficient | 0.2 |
| | Static friction coefficient | 0.8 |
| | Dynamic friction coefficient | 0.01 |
| Rice grain-Variable amplitude screening mechanism | Restitution coefficient | 0.5 |
| | Static friction coefficient | 0.7 |
| | Dynamic friction coefficient | 0.01 |
| Rice stem-Rice stem | Restitution coefficient | 0.2 |
| | Static friction coefficient | 0.8 |
| | Dynamic friction coefficient | 0.01 |
| Rice stem-Variable amplitude screening mechanism | Restitution coefficient | 0.2 |
| | Static friction coefficient | 0.8 |
| | Dynamic friction coefficient | 0.01 |

### 2.4 Simulation test scheme

0.5 kg/s was selected as the abnormal constant feeding rate for testing. When the feeding quantity of the materials increased, the angle of the guide chute at the front end of the screen surface was adjusted, the amplitude and vibration direction angle at screen surface were changed for positions, and the simulation test of the variable amplitude anti-blocking screening process was performed. The Grad Bin Group of EDEM was implemented to divide the screen surface into several grids along the length direction and subsequently derive the material distribution on the screen surface

with variable amplitudes at different times. Then the distribution of the material backward movement on the screen surface was analyzed with variable amplitude under different guide chute angles. Table 4 reports the simulation test scheme for the anti-blocking of the variable amplitude screen surface.

**Table 4 Test scheme for the anti-blocking of a variable amplitude with increasing material feeding.**

| Order number | Guide chute angle/(°) |
|---|---|
| 1 | 0 |
| 2 | 5 |
| 3 | 10 |
| 4 | 15 |
| 5 | 20 |
| 6 | 25 |
| 7 | 30 |
| 8 | 35 |
| 9 | 40 |
| 10 | 45 |

### 2.5 Simulation data

The Grid Bin Group of EDEM was employed to divide the screen surface of the variable amplitude screening mechanism into 10 grid areas along the length direction (from the screen front to rear) in Figure 4, named as Grid 1-10 respectively. Under the changing material feeding quantity (abnormal constant feeding: 0.5 kg/s) and different guide chute angles (variable amplitude adjustment), the material quality change was determined in the screen surface grid areas across different times. The vibration frequency of the variable amplitude screening mechanism was 5 Hz, the movement was completed in 0.2 s, and data was collected every 0.1 s. The material distribution changes in the screen surface grid areas under different guide chute angles were then derived. Table 5 reports the material quality changes in 10 example grid areas of the screen surface at the guide chute angle of 5°.

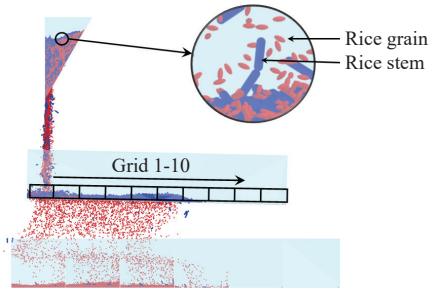


Figure 4 Schematic diagram of simulation processing.

**Table 5 Material quality distribution in different screen surface grid areas (guide chute angle: 5°).**

| Order number | Time/s | Grid 1/kg | Grid 2/kg | Grid 3/kg | Grid 4/kg | Grid 5/kg | Grid 6/kg | Grid 7/kg | Grid 8/kg | Grid 9/kg | Grid 10/kg |
|---|---|---|---|---|---|---|---|---|---|---|---|
| 1 | 2.60 | 0.00 | 0.00 | 0.00 | 0.00 | 0.00 | 0.00 | 0.00 | 0.00 | 0.00 | 0.00 |
| 2 | 2.70 | 0.00 | 0.00 | 0.00 | 0.00 | 0.00 | 0.00 | 0.00 | 0.00 | 0.00 | 0.00 |
| 3 | 2.80 | 0.00 | 0.00 | 0.00 | 0.00 | 0.00 | 0.00 | 0.00 | 0.00 | 0.00 | 0.00 |
| 4 | 2.90 | 0.04 | 0.01 | 0.00 | 0.00 | 0.00 | 0.00 | 0.00 | 0.00 | 0.00 | 0.00 |
| 5 | 3.00 | 0.06 | 0.03 | 0.00 | 0.00 | 0.00 | 0.00 | 0.00 | 0.00 | 0.00 | 0.00 |
| 6 | 12.10 | 0.05 | 0.04 | 0.02 | 0.00 | 0.00 | 0.00 | 0.00 | 0.00 | 0.00 | 0.00 |
| 7 | 12.20 | 0.04 | 0.05 | 0.03 | 0.00 | 0.00 | 0.00 | 0.00 | 0.00 | 0.00 | 0.00 |
| 8 | 12.30 | 0.05 | 0.04 | 0.02 | 0.00 | 0.00 | 0.00 | 0.00 | 0.00 | 0.00 | 0.00 |
| 9 | 12.40 | 0.04 | 0.05 | 0.03 | 0.00 | 0.00 | 0.00 | 0.00 | 0.00 | 0.00 | 0.00 |
| 10 | 12.50 | 0.05 | 0.04 | 0.02 | 0.00 | 0.00 | 0.00 | 0.00 | 0.00 | 0.00 | 0.00 |

### 2.6 Establishment of BP neural network model

The BP neural network (BPNN) is a multilayer feedforward neural network trained according to the error back propagation algorithm. It is composed of input, output and hidden layers and searched by gradient descent method (along the gradient descending direction to approach minimum deviation) in order to minimize the error mean square deviation of the actual and expected output values of the network[35]. The BP neural network has a strong nonlinear mapping ability, which can automatically extract the "reasonable rules" between input and output data through learning, and has strong self-adaptive and self-learning capabilities. The BP neural network is currently the most widely used neural network plays an important supporting role in agricultural intelligence.

The BP neural network model was designed using Matlab2017a (MathWorks). The rotation angle of the guide chute, feeding quantity and time were taken as the input layers in BP neural network model. Each input layer had three nodes and each grid area on the variable amplitude screen surface was taken as the output layer. The number of nodes in the output layer was set to 10. The basic principle for selecting the number of nodes in the hidden layer was to select between the number of nodes in the input and output layers, which was approximately two-thirds of the sum of the number of input and output layers. Therefore, the number of nodes in the selected hidden layer was 8, 9 and 10 respectively. The BP neural network model was trained with different numbers of hidden layer nodes. When the number of neurons in the hidden layer was determined as 10, the gradient of the BP neural network model decreased rapidly, the error was small and the fitting accuracy was high.

Due to the large number of samples, the training, verification, and test set samples of the BP neural network model were randomly selected according to the proportion 80% : 10% : 10% with the aim of increasing the number of training samples, and ultimately improving the training model accuracy. The Levenberg Marquardt function, a nonlinear optimization approach based on the Newton and gradient descent methods, was selected as the training function. The gradient and Newton methods are the most widely used nonlinear least square algorithms. The former is fast and has a short training time, yet it consumes a lot of computer memory. Therefore, a high-performance workstation was employed to build and train the BP neural network model, allowing for a short completion time. The weights and thresholds of the BP neural network model were set as the default values, and the default learning function was used to establish the adjustment rules. Figure 5 depicts the BP neural network structure built using Matlab2017a (MathWorks).

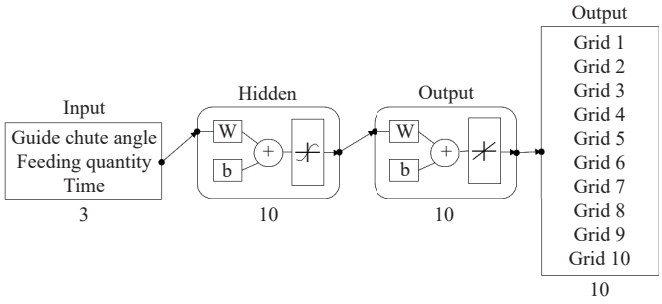


Figure 5 BP neural network structure designed based on Matlab

## 3 Results and analysis

### 3.1 Simulation process and results

Figure 6 depicts the anti-blocking simulation process of the variable amplitude screen surface under the abnormal and constant feeding of materials (0.5 kg/s). Considering the dynamic changes of the material feeding quantity in the subsequent tests, a particle factory above the hopper was established to dynamically generate particles for material filling, and controlled the baffle to move a certain distance in RecurDyn, hence changing the material feeding quantity. The rice grain and stem particles continuously collided with the screen surface during the simulation process, and penetrated and moved backward with the movement of the variable amplitude screening mechanism. The amplitude of the screen surface front end increased with the guide chute angle, as did the local throwing strength of the materials, while the materials at the front end of the screen surface accelerated backwards. This effectively alleviated the accumulation and blockage of the materials at the front end of the screen surface and achieved the

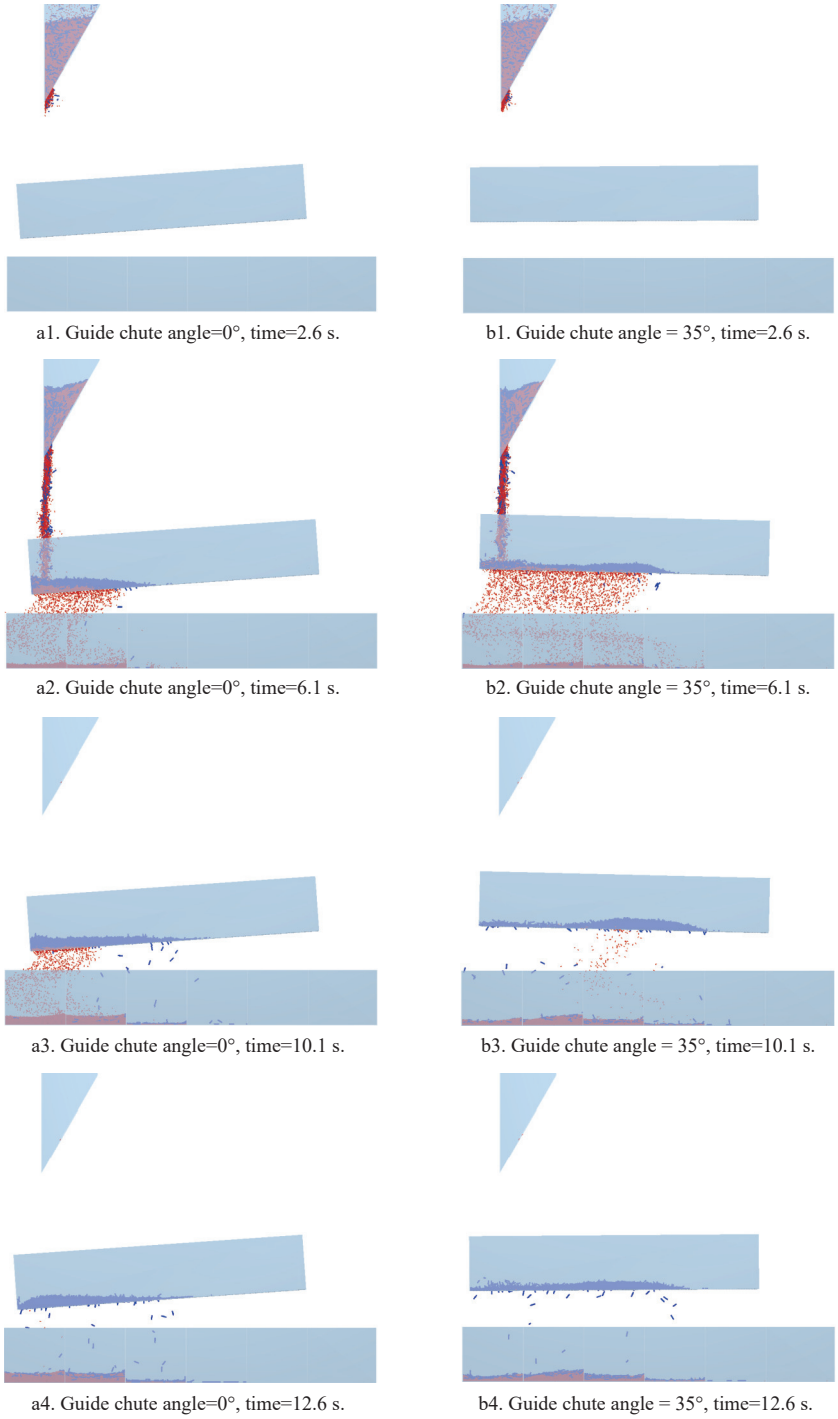

a1. Guide chute angle=0°, time=2.6 s. b1. Guide chute angle = 35°, time=2.6 s.

a2. Guide chute angle=0°, time=6.1 s. b2. Guide chute angle = 35°, time=6.1 s.

a3. Guide chute angle=0°, time=10.1 s. b3. Guide chute angle = 35°, time=10.1 s.

a4. Guide chute angle=0°, time=12.6 s. b4. Guide chute angle = 35°, time=12.6 s.

Figure 6 Simulation screening process of rice grain and stem under different variable amplitude regulation.

normal screening of the materials.

At the guide chute angle of 0°, the variable amplitude screening mechanism was in the form of a reciprocating vibrating screen (Figure 6a). As the simulation proceeded, the materials on the screen surface were generally concentrated at the front screen surface for screening. Such conditions are likely to exceed the upper load limit of the vibrating screen for the continuous feeding of materials under changing quantities (abnormal constant feeding: 0.5 kg/s). This can cause the accumulation and blockage of materials at the front end of the screen surface and affect the normal material screening progress. At the guide chute angle of was 35°, the material quickly moved back to the middle area of the screen surface within a period (2.6-6.1 s) when it fell to the front end of the screen surface (Figure 6b). As the simulation progressed, the materials were generally concentrated in the center of the screen surface for screening. Comparing the guide chute angles of 35° and 0° reveals a reduction in the material quantity at the screen surface front end during the guide chute angles of 35°, effectively alleviating the accumulation and blockage of the screen surface caused by the increased feeding quantity, and shorting the screening time of the changed feeding quantity.

### 3.2 BP neural network training results and analysis

The BP neural network model was used to train randomly selected samples several times. The R of each training exceeded 0.96. The best training results (the R and the error) were selected to establish the BP neural network prediction model. Figure 7 presents the mean square error (MSE), error histogram and regression curve of the model. When the training reached 76 steps, the MSE of the training, verification, and test sets converged to a lower level, with a rapid convergence speed Figure 7a. The error difference between the predicted and output values of the training, verification, and test sets was small, and the error followed a normal distribution (Figure 7b), with error values generally concentrated between –0.009 05 to 0.009748. The error difference distribution was relatively concentrated near the zero line, with error values approximately 0.000348. This indicates small errors between the BP predicted data and output values, as well as a high fitting degree. Furthermore, the correlation between the predicted and output values of the training, verification, and test sets exceeded 0.97 (Figures 7c-7f). This reveals the closeness between the BP neural network model predictions and the simulation values, with the BP neural network prediction model demonstrating a high reliability. The changes in the screen surface material distribution with variable amplitude were predicted by the BP neural network model and compared with the equivalent simulation values. This verified the accuracy and reliability of the BP neural network training model in predicting the screen surface material distribution.

### 3.3 Prediction material distribution model results and analysis

Figure 8a depicts the changes in the screen surface material distribution of the variable amplitude screening process under different guide chute angles simulated by the EDEM-RecurDyn model. The continuous increase in the guide chute angle resulted in a reduction in the material quality of Grid 1, 2 and 3 at the screen surface front end, while that of Grid 4, 5, 6 and 7 gradually increased, and the materials on the screen surface were evenly distributed. The time taken for the accumulation and retention of materials at the screen surface front end decreased (particularly for materials in Grid 1-3) with the increasing guide chute angle. This is because the greater guide chute angle (variable amplitude adjustment) enhanced the amplitude at the screen surface front end, which accelerated backward movement of materials, and they thus no longer accumulated at the front end. However, at the guide chute angles of 40°-45°, some of the material fell into the rear area of the screen surface during the screening, and it could be predicted that the materials would be discharged from the vibrating screen with the vibration of the screen surface over time. This had an adverse impact on the screening performance.

At the guide chute rotation angles of 0°-15°, the backward moving speed of the material was slow, the backward moving mass of the material was small, with an extensive retention time of the material at the screen surface front end (Figures 8a1-8a4; Figures 8b1-8b4). At around 8 s, the material began to approach Grid 5. The variable amplitude adjustment (guide chute angles of 0°-15°) did not have any obvious effect on relieving the accumulation and blockage of the material on the screen surface. At the guide chute angles of 20°-25°, the backward movement effect of the material on the screen surface began to appear, and the material on the screen surface reached Grid 6 in approximately 6 s. At this time, the materials on the screen surface were evenly distributed (Figures 8a5-8a6; Figures 8b5-8b6). The variable amplitude adjustment was observed to alleviate the material accumulation and blockage at the front end of the screen surface to some extent. At the guide chute angles of 30°-40°, the materials were maintained at the screen surface front for a sort time (Figures 8a7-8a9; Figures 8b7-8b9). At around 4 s, the materials on the variable amplitude screen surface were evenly distributed in Grid 1-6 and the backward movement effect of the screen surface materials under the variable amplitude adjustment (relative to other guide chute angles) improved. However, as the material screening time progressed, the screen surface materials at the guide chutes angle of 30° were generally maintained in Grid 1-6 for screening. This was conductive to avoiding the blocking of the variable amplitude screen surface and for material screening. The screen surface material under the guide chute angle of 40° began to gradually move to Grid 7-9 in the rear region of the vibrating screen. This may lead to the material being discharged from the rear part of the vibrating screen during the screening, which can have a serious impact on the screening performance, namely a decline in the screening efficiency and a continuous increase in the loss rate. At the guide chute angle of 45°, the material at the screen surface front end reached Grid 6 in 3 s, with an obvious backward moving effect (Figures 8a10 and 8b10). However, as the time progressed, the materials on the screen surface also began to move towards Grid 7-10 and the materials moved further backwards. This variable amplitude adjustment is thus not desirable. The screening and anti-blocking time under the guide chute angle of 45° should be controlled according to the change of material feeding quantity. For example, when the feeding quantity is 0.5 kg/s, the screening and anti-blocking time should not exceed 3 s.

At the guide chute angles of 20°-40°, the materials at the front end of the screen surface were evenly distributed in Ggrid1-6 within 3-6 s. Under small guide chute angles, a longer time was required for the material to move back (Figures 8a1-8a3; Figure 8b1-8b3), indicating the long time taken to alleviate the accumulation and blockage of the screen surface. Again, this is not desirable. It aimed to quickly move the materials back to the vicinity of Grid 6 (not passing Grid 7), such that they were able to make full use of the front and middle screen surface (Grid 1-6) for screening. This could better alleviate the problem of material accumulation and blockage at the front end of the screen surface. Therefore, the angle and time of the guide chute need to be regulated. When the material feeding quantity changed (abnormal and constant feeding: 0.5 kg/s), the optima guide chute angle was 20°-45°, with a regulation time of 3-

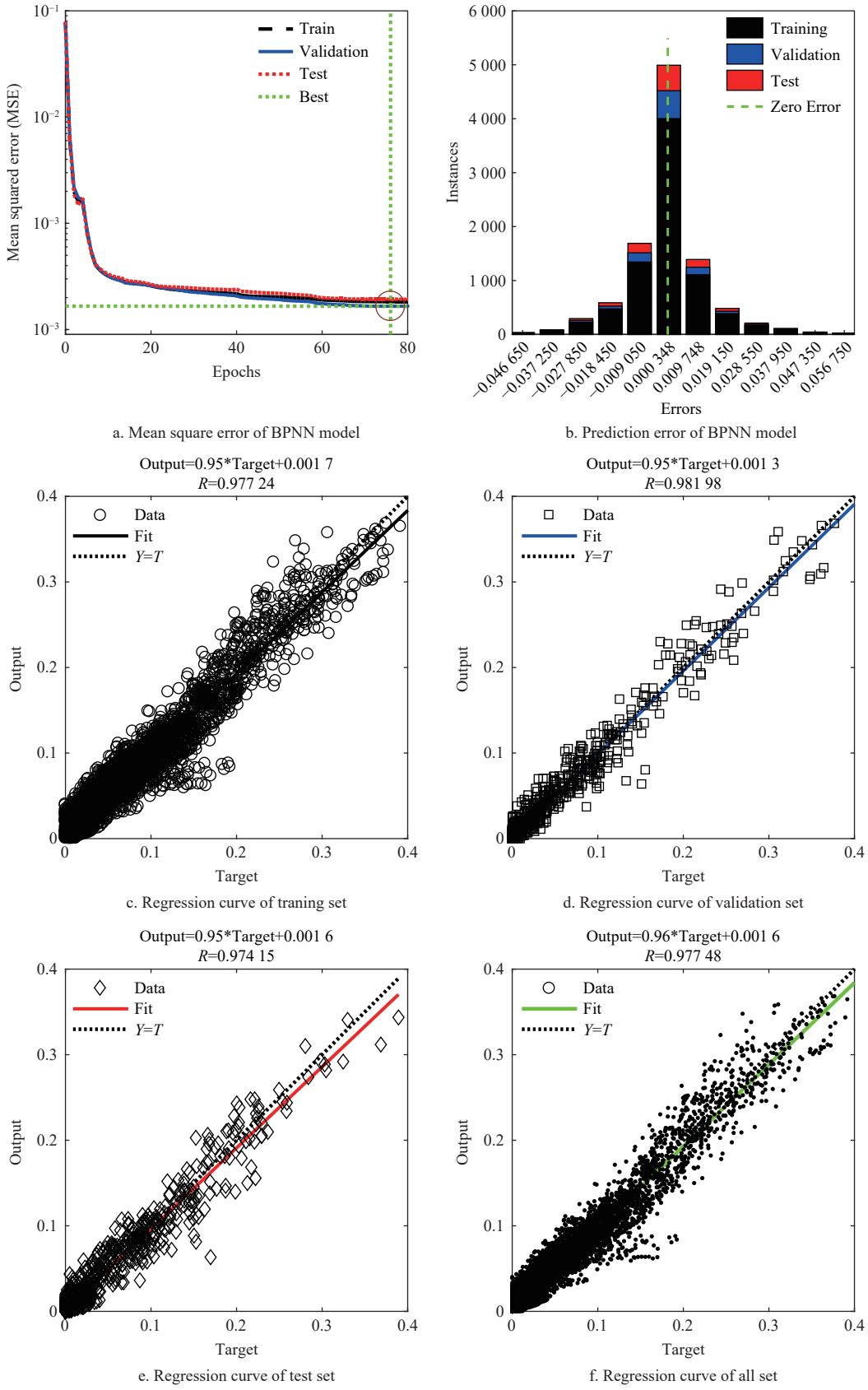


a. Mean square error of BPNN model

b. Prediction error of BPNN model

c. Regression curve of traning set

d. Regression curve of validation set

e. Regression curve of test set

f. Regression curve of all set

Figure 7 Training processes and results of the BP neural network model based on Matlab

6 s. At this time, the materials at the screen surface front end were able to move quickly back to the vicinity of the Grid 6 to alleviate the accumulation and blockage of the material.

Figure 8b presents the material distribution diagram of the variable amplitude screen surface predicted by the BP neural network model. The change trends of the variable amplitude screen surface material distributions in Figures 7a and 7b are essentially consistent. As the vibration frequency of the vibrating screen was 5 Hz, the variable amplitude screening mechanism completed its movement every 0.2 s and collected the material quality in different grid areas every 0.1 s. Therefore, the material distribution diagram of the variable amplitude screen surface obtained from the

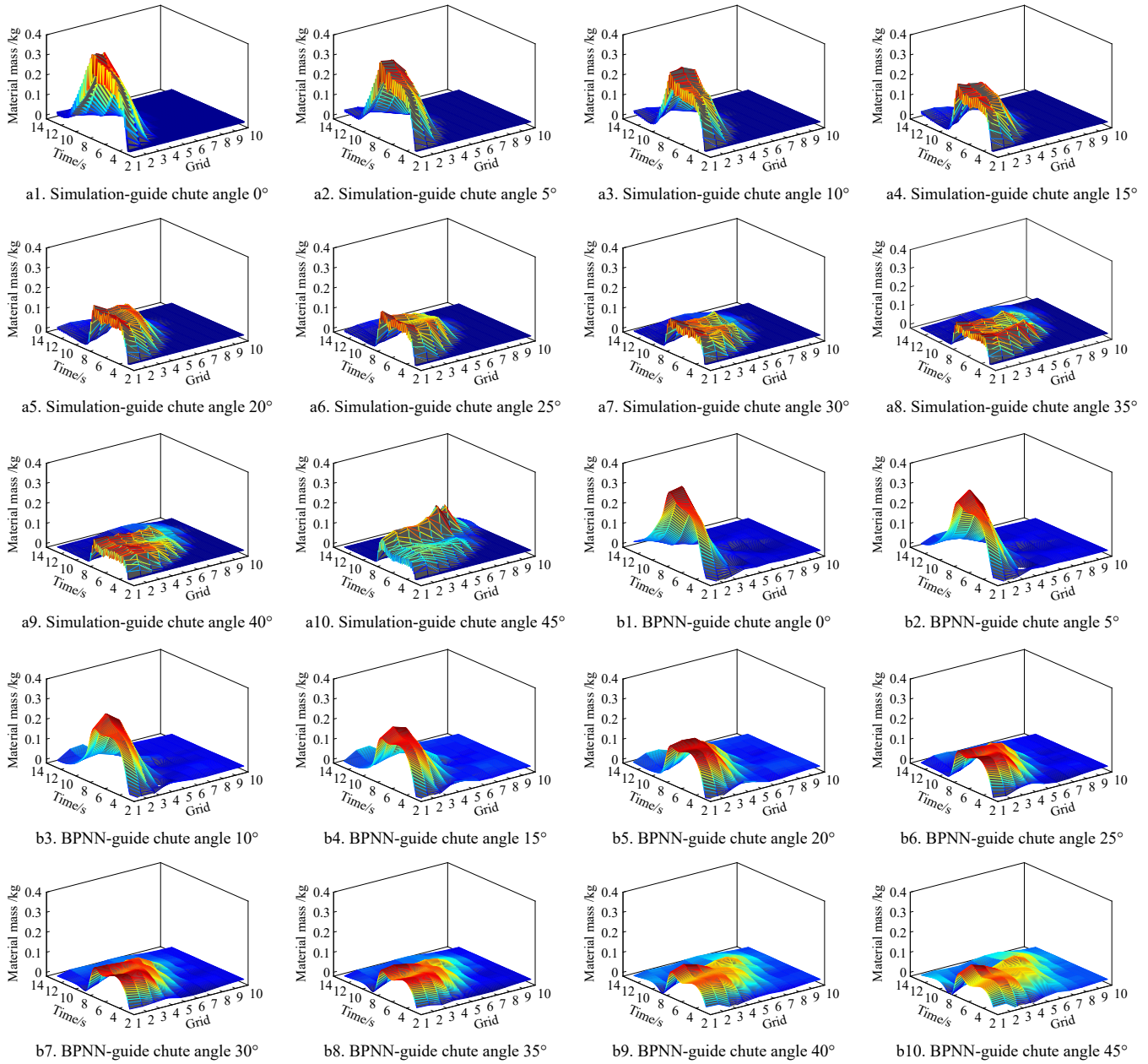


a1. Simulation-guide chute angle 0° a2. Simulation-guide chute angle 5° a3. Simulation-guide chute angle 10° a4. Simulation-guide chute angle 15°

a5. Simulation-guide chute angle 20° a6. Simulation-guide chute angle 25° a7. Simulation-guide chute angle 30° a8. Simulation-guide chute angle 35°

a9. Simulation-guide chute angle 40° a10. Simulation-guide chute angle 45° b1. BPNN-guide chute angle 0° b2. BPNN-guide chute angle 5°

b3. BPNN-guide chute angle 10° b4. BPNN-guide chute angle 15° b5. BPNN-guide chute angle 20° b6. BPNN-guide chute angle 25°

b7. BPNN-guide chute angle 30° b8. BPNN-guide chute angle 35° b9. BPNN-guide chute angle 40° b10. BPNN-guide chute angle 45°

Figure 8 Comparison of variable amplitude screen surface material distributions under simulation and BPNN prediction

simulation test presented a sawtooth shape across time. Moreover, the material distribution diagram of the variable amplitude screen surface predicted by the BP neural network training model was relatively smooth.

Comparing Figures 8a and 8b reveals a high fitting degree between the BP-predicted and simulated screen surface material distribution for the area with the most material on the variable amplitude screen surface. The area with less material (dark blue area in Figure 8) was associated with a certain error in the BP-precited screen surface material distribution (i.e., the difference between zero values and small negative values, with errors mainly concentrated around –0.001 09, Figure 7b). This had minimal impact on the material distribution on the variable amplitude screen surface. Therefore, the fitting degree between Figure 8a and 8b was very high, indicating the reliability of the BP neural network prediction model. This verified the feasibility and accuracy of the BP neural network for predicting the varying material distribution in different grid areas of the variable amplitude screen surface, and provides a part of the basis to establish the regulation model of variable amplitudes under changes in material feeding.

## 4 Conclusions

In this study, the guide chute rotation angles were selected as the variable, the process of variable amplitude screening and anti-blocking under a changing feeding quantity was simulated based on EDEM-RecurDyn, and the prediction model of the material distribution on the screen surface under different variable amplitude was constructed by the BP neural network.

The results indicated that the material accumulation mass and time at the front end of the variable amplitude screen surface decreased with the increasing guide chute angle. Under the abnormal feeding rate of 0.5 kg/s, the angle and adjustment time of the guide chute should be controlled at 20°-45° and 3-6 s respectively, such that the material at the front end of the screen surface can quickly move back to the center of the screen surface. The angle of the guide chute was 30°-35°, and the materials at the front of the variable amplitude screen surface were evenly distributed in grid areas 1-6 within just 4 s, with more favorable screen surface anti-blocking effect.

The R values of BP neural network model exceeded 0.97,

which indicated the higher accuracy. This provides an important basis for the prediction and analysis of the material distributions for screen surfaces with variable amplitudes. In particular, the variable amplitude can be adjusted to alleviate the accumulation and blockage of the material on the screen surface, facilitating the intelligent control of the material on screen surfaces with variable amplitude.

Predicting the material distribution on the screen surface through a BP neural network allows us to determine the adjustment size and time of the guide chute angle. This provides a basis for establishing variable amplitude adjustment strategy. The proposed approach has great potential. In the future, additional variable amplitude adjustment data (more abnormal feeding rate of the threshed mixture) are required for accurate predictions and analysis, so as to establish an intelligent control strategy and model with variable amplitude that can better alleviate the accumulation and blockage of the material on the screen surface.

## Acknowledgements

This work was supported financially by National Natural Science Foundation of China (Grant No. 51975256, 52375249), Jiangsu Province and Education Ministry Co-sponsored Synergistic Innovation Center of Modern Agricultural Equipment (Grant No. XTCX2011), Jiangsu Modern Agricultural Machinery Equipment and Technology Demonstration and Promotion Project (Grant No. NJ2021-07), a project funded by the Priority Academic Program of the Development of Jiangsu Higher Education Institutions (PAPD).

## [References]

[1] Wang L J, Song L L, Feng X, Wang H S, Li Y H. Research status and development analysis of screening devices of grain combine harvester. Transactions of the CSAM, 2021; 52(6): 1–17.

[2] Li H B, Zhao X Q, Geng K H. Design and analysis on configuration of a multiple DOF and rigid-flexible coupling sieving machine. Mining & Processing Equipment, 2020; 48(4): 46–50. (in Chinese)

[3] Chang J, Wang C J, Hu Z B, Han D D, Chen L. Design of a variable degree of freedom parallel vibration sieve. Mechanical Engineering & Automation, 2015(4): 97–99+102. (in Chinese)

[4] Li J. Research of three-dimensional parallel vibration screen for grain cleaning. PhD dissertation, Zhenjiang: Jiangsu University, 2013; 133p. (in Chinese)

[5] Bao C Y. Study on vibrating screening process mechanism basing on DEM. MA thesis. Xuzhou: China University of Mining and Technology, 2016; 96p. (in Chinese)

[6] Wang Z Y, Ren N, Wu W B, Li Y X. Research on screening results of reciprocating vibration screen based on discrete element method. Journal of Agricultural Mechanization Research, 2016; 38(1): 33–38. (in Chinese)

[7] Ma Z, Li Y M, Xu L Z. Discrete-element method simulation of agricultural particles' motion in variable-amplitude screen box. Computers and Electronics in Agriculture, 2015; 118: 92–99.

[8] Zeng Z W, Ma X, Cao X H, Li Z H, Wang X C. Critical review of applications of discrete element method in agricultural engineering. Transactions of the CSAM, 2021; 52(4): 1–20. (in Chinese)

[9] Ma Z, Li Y M, Xu L Z, Chen J, Zhao Z, Tang Z. Dispersion and migration of agricultural particles in a variable-amplitude screen box based on the discrete element method. Computers and Electronics in Agriculture, 2017; 142: 173–180.

[10] Li H, Wang J S, Yuan J B, Yin W Q, Wang Z M, Qian Y Z. Analysis of threshed rice mixture separation through vibration screen using discrete element method. Int J Agric & Biol Eng, 2017; 10(6): 231–239.

[11] Ma X D, Zhao L, Guo B, Dang H. Simulation and experiment of rice cleaning in air-separation device based on DEM-CFD coupling method. Int J Agric & Biol Eng, 2020; 13(5): 226–233.

[12] Wu X J, Li S Y, Fang P, Xi Z J, Hou Y J, Liu Y P. Particle migration DEM simulation of shale shaker under different screen surface shape. Mechanical Research & Application, 2017; 30(5): 45–49. (in Chinese)

[13] Harzanagh A A, Orhan E C, Ergun S L. Discrete element modelling of vibrating screens. Minerals Engineering, 2018; 121: 107–121.

[14] Van Xo N, Linh N K. Applications of Discrete Element Method (DEM) in modeling the impact of dynamic and technological parameters on the material movement on the vibrating screen surface//IOP Conference Series: Materials Science and Engineering. IOP Publishing, 2020; 843(1): 012024.

[15] Xu Y F, Zhang X L, Wu S, Chen C, Wang J Z, Yuan S Q, et al. Numerical simulation of particle motion at cucumber straw grinding process based on EDEM. Int J Agric & Biol Eng, 2020; 13(6): 227–235.

[16] Zhang J, Liu F Y, Chen J. Virtual vibration screening experiments of grain cleaning sieve based on DEM. Journal of Agricultural Mechanization Research, 2019; 41(2): 187–191. (in Chinese)

[17] Ji L L, Xie H X, Yang H G, Wei H, Yan J C, Shen H Y. Simulation analysis of potato dry soil cleaning device based on EDEM-RecurDyn coupling. Journal of Chinese Agricultural Mechanization, 2021; 42(1): 109–115. (in Chinese)

[18] Wen P F, Qiao J P, Duan C L, Jiang H S, Zhao Y M. Research on Screening Behavior and Distribution of Materials during Variable Amplitude Equal Thickness Screening. Coal Mine Machinery, 2020; 41(4): 165–167. (in Chinese)

[19] Jiang H S. Research on the Mechanism of Variable-amplitude Equal-thickness Elastic Deep Screening of Moist Coal. Xuzhou: China University of Mining and Technology, 2017; 166 p. (in Chinese)

[20] Zhu N Y, Liu X, Liu Z Q, Hu K, Wang Y K, Tan J L, et al. Deep learning for smart agriculture: Concepts, tools, applications, and opportunities. Int J Agric & Biol Eng, 2018; 11(4): 32–44.

[21] Huang Y B. Research status and applications of nature-inspired algorithms for agri-food production. Int J Agric & Biol Eng, 2020; 13(4): 1–9.

[22] Zhang Q. Research and application of BP neural network in agricultural engineering. Agricultural Engineering, 2012; 2(5): 17–20. (in Chinese)

[23] Wang J Q. Research on BP neural network theory and its application in agricultural mechanization. PhD dissertation, Shenyang: Shenyang Agricultural University, 2011; 115p. (in Chinese)

[24] Hu J, Xin P P, Zhang S W, Zhang H H, He D J. Model for tomato photosynthetic rate based on neural network with genetic algorithm. Int J Agric & Biol Eng, 2019; 12(1): 179–185.

[25] Li T, Zhang M, Ji Y H, Sha S, Jiang Y Q, Li M Z. Management of $CO_2$ in a tomato greenhouse using WSN and BPNN techniques. Int J Agric & Biol Eng, 2015; 8(4): 43–51.

[26] Feng X B, He P J, Zhang H X, Yin W Q, Qian Y, Cao P, et al. Rice seeds identification based on back propagation neural network model. Int J Agric & Biol Eng, 2019; 12(6): 122–128.

[27] Shanmugam B K, Vardhan H, Raj M G, Kaza M, Sah R, Hanumanthapp.H. Artificial neural network modeling for predicting the screening efficiency of coal with varying moisture content in the vibrating screen. International Journal of Coal Preparation and Utilization, 2021; 1–19.

[28] Li X, Sun X Y, Li L Y. Optimization design of angular velocity control of threshing cylinder in combine harvester based on wavelet neural network. Journal of Agricultural Mechanization Research, 2016; 38(11): 64–68. (in Chinese)

[29] Ge Y S, Zhou D D, Xu R. Research on loss detection of combine harvester based on neural network. Journal of Nanjing Institute of Technology (Natural Science Edition), 2018; 16(2): 57–61. (in Chinese)

[30] Song B C, Liu C S, Cheng J, Hu M. Optimization of parameters for wet phosphate rock screening based on neural network and DEM technology. Industrial Minerals & Processing, 2016; 45(9): 6–8. (in Chinese)

[31] Zhao Z, Jin M Z, Qin F, Yang S X. A novel neural network approach to modeling particles distribution on vibrating screen. Powder Technology, 2021; 382: 254–261.

[32] Kim K C, Jiang T, Kim N I, Kwon C. Effects of ball-to-powder diameter ratio and powder particle shape on EDEM simulation in a planetary ball mill. Journal of the Indian Chemical Society, 2022; 99(1): 100300.

[33] Ma L R, Cao S K, Zhong W Z, Song X W, Shen H. Simulation research on operation parameters of cleaning device based on EDEM. Agricultural Technology & Equipment, 2017; 7: 80–83. (in Chinese)

[34] Li H C. Theoretical and experimental study on air -and -screen cleaning unit. PhD dissertation. Zhenjiang: Jiangsu University, 2011; 119p. (in Chinese)

[35] Zhang C, Guo Y, Li M. Review of development and application of artificial neural network models. Computer Engineering and Applications, 2021; 57(11): 57–69. (in Chinese)